A FTIR Characterization of Surface Interactions of Cyanide and Coppercyanide with a Platinum Electrode in Alkaline Solution

R.M. Souto[a], F. Ricci[b], L. Szpyrkowicz[b], J.L. Rodríguez[a] and E. Pastor[a]

[a] Department of Physical Chemistry, University of La Laguna, 38071 La Laguna, Tenerife, Canary Islands, Spain. (fax:+34922318002; e-mail: rsouto@ull.es)

[b] Department of Environmental Sciences, University of Venice, 30123 Venice, Italy (fax:+390412348591; e-mail: lidia@unive.it)

Abstract

In this paper, the nature of the species formed in the electrochemical interactions between a polycrystalline platinum surface and cyanide and copper-cyanide species in alkaline solution (pH 13) has been investigated by combining cyclic voltammetry with in situ FTIR spectroscopy. This study was performed because electrochemical reactors for the treatment of cyanide-containing industrial wastewaters have been shown to achieve viable destruction rates when copper ions are present in the alkaline solution through the formation of copper oxide films [1-3]. It has been found that the complexation of cyanide ions by copper species hinders the adsorption of the anion at the electrode, thus avoiding the characteristic electrode poisoning by CO that occurs in the absence of soluble copper species. Conversely, soluble copper-cyanide complexes can be electrooxidized at the platinum surface through the formation of cyanate species as intermediate, and of HCOOH and NO as end products. The addition of copper species to the electrolyte also facilitates this route for cyanide oxidation to occur at higher rates without poisoning the platinum electrode.

Keywords: FTIR; voltammetry; platinum; cyanide oxidation; copper ions; catalysis.

1. Introduction

Cyanide species are widely employed in a variety of technological processes including mining, metal and mineral processing, electroplating and metal finishing, due to their unmatched characteristics for the selective complexation of metal ions [1]. Cyanide species are also encountered in oil refineries, in chemical manufacturing plants and in thermoelectric power stations [2], thus becoming a frequent chemical in our technological society. On the other hand, cyanide solutions are characterized by their high biological toxicity [3] and very low degradability by conventional treatments [4,5]. These treatments generally consist in the oxidation of cyanide species, and the subsequent precipitation of metal ions as hydroxides, but they involve both the use of volatile toxic oxidants, and the resulting sludges are difficult to handle [6]. Additionally, the presence of concomitant copper in some of the industrial operations (cf. gold leaching or copper plating, etc.) results in the generation of copper cyanide which creates significant additional hazardous waste [7].

An attractive alternative for the treatment of cyanide by oxidation, which additionally allows for the simultaneous recovery of dissolved metal ions, is based in the application of electrochemical reactors [8-17]. However, on many electrode materials, the electrochemical oxidation of uncomplexed cyanides is kinetically limited and inhibited by adsorbed species [18]. Hence, to achieve viable destruction rates, research has been directed towards the discovery of electrocatalytic processes for the oxidation of cyanide. Such catalytic effects have been observed when either the anode in the electrochemical cell was previously covered with a copper oxide layer [19-22], or copper ions were present in the solution [23-27]. In this later case, formation of copper oxide films were also observed in the anode simultaneously to copper deposition at the cathode of the electrochemical reactor [18,28-31]. The formation of this copper oxide covered electrode surface has been then regarded to be a necessary step to facilitate the oxidation of cyanide [12,21,28], though different mechanisms have been proposed for such an effect [18]. Conversely, some authors claim that the catalytic effect towards cyanide oxidation arises from a heterogeneous mechanism through adsorbed cyanic species [23,30,32,33].

Though there have been numerous studies on the adsorption and oxidation of cyanide on different metals, such as gold, silver, platinum and palladium, they were undertaken only as a part of descriptions of molecular adsorption from copper-free aqueous solutions [34-41]. Only a few studies on the electrochemical processes occurring in copper-cyanide solutions have been published until now [30,33], but they lack information at a molecular level since they relied on information from conventional electrochemical techniques. Thus, specific studies of the adsorption and oxidation of copper cyanide solutions by using spectroelectrochemical techniques

are needed.

2. Experimental

Analytical grade sodium cyanide, cuprous cyanide and sodium hydroxide (Merck) were used as received. Deionized (Millipore Milli-Q*, 18 mΩ cm) water was used for the preparation of all solutions. The base electrolyte was prepared by adding NaOH to deionized water until pH 13 was reached. The total cyanide concentration in the solutions was 31 mM, which was attained by combining different amounts of KCN and CuCN [18]. Measurements were conducted at room temperature (21 ± 1ºC), and the spectroelectrochemical cell was purged with argon (99.998%, Air Liquide) prior to each experiment.

The IR spectroelectrochemical technique employed was Fourier transform infrared spectroscopy (FTIR). Instrumentation and experimental arrangements have been described in detail previously [42,43]. Briefly, spectra were collected with a Bruker Vector 22 spectrometer equipped with a MCT detector. An IR cell fitted with a 60º CaF_2 prismatic window at its bottom was employed. For each spectrum, 100 scans were collected at a resolution of 8 cm^{-1}. Parallel (p) and perpendicular (s) polarized IR light was obtained from a BaF_2 supported Al grid polarizer. Spectra are plotted as the reflectance ratio R/R_0, where R and R_0 are the reflectances corresponding to the sample and the reference potential, respectively. Electrode potentials were controlled with a Heka PG310 potentiostat system and a reversible hydrogen electrode (RHE) in the supporting electrolyte as a reference electrode. The working electrode was a polycrystalline Pt disk (0.785 cm^2 geometric area), and a platinum sheet was used as counter electrode. The Pt electrode was pretreated immediately prior to use by cycling at 0.05 V s^{-1} between 0.05 and 1.50 V versus RHE in the base electrolyte.

3. Results and discussion

3.1. Voltammetric characterization of the electrochemical behaviour

The stationary cyclic voltammogram (CV) measured in the spectroelectrochemical cell at 50 mV s^{-1} for the polycrystalline platinum electrode immersed in a cyanide-free alkaline solution at pH 13 is depicted in figure 1A. It shows peaks due to hydrogen adsorption-desorption processes at applied potentials more negative than 0.4 V (RHE), while the broad wave observed at potential values more positive than 0.6 V (RHE) during the positive-going potential scan is due to the formation of a surface oxide layer. This oxide layer can be stripped off during the corresponding negative-going potential scan for applied potentials below 0.9 V (RHE). A more detailed

description of these processes at the platinum electrode in an alkaline aqueous solution can be found in the literature [44-46].

The shape of the stationary CV is modified in a very major extent when cyanide ions are present in the electrolytic solution, as shown in figure 1B. It can be observed that cyanide prevents hydrogen adsorption in the negative potential regime, and suppresses to a great extent the formation of surface oxide. In this solution, no visible oxidation wave can be seen at the platinum electrode up to the onset of oxygen evolution at potential values above 1.2 V (RHE). Nevertheless, the onset of a small oxidation current is observed at ca. 0.5 V (RHE), which grows slowly until the potential of oxygen evolution, which may be evidence for oxide formation. Anyway, the current involved in oxide formation is significantly smaller than for the cyanide-free case (cf. figure 1A), which is confirmed by the clear decrease of the charge under the reduction peak in the subsequent negative-going potential scan.

The influence of copper(I) ions on the electrochemical behaviour of the system is easily concluded from the inspection of the CV plotted in figure 1C. It was measured after adding Cu(I) in a solution which contained the same total cyanide concentration as in the previous case. It is clear that the presence of Cu(I) enhanced the oxidation current at potential values higher than 0.7 V (RHE), describing a defined oxidation peak centred at ca. 0.93 V (RHE), and the anodic current starts to grow steadily when the potential value 1.0 V (RHE) is passed. On the reverse scan, the reduction peak previously ascribed to the reduction of a surface oxide layer is clearly observed as for the corresponding CV measured in the cyanide-free solution in figure 1A. In fact, the charge under this peak is similar in both cases, thus indicating that the formation of the oxide film on platinum is not hindered by cyanide ions when Cu(I) species are also present in the medium. Therefore, copper-cyanide complexes are more effectively oxidized on platinum than cyanide ions, and Cu(I) species maybe regarded as a catalyst for the process.

3.2. FTIR spectra in a copper-free alkaline solution containing cyanide ions

In situ IR spectroelectrochemical data of the platinum + cyanide system in alkaline sodium hydroxide solution are shown in figures 2 and 3. The FTIR spectra arising from both s- and p-polarized radiation were determined to distinguish adsorbed species from those in the solution. The spectra were acquired by applying 0.05 V single potential steps from the reference potential (E_0 = 0.05 V (RHE)) first in the positive-going direction up to 1.5 V (RHE) (figures 2A and 3A), and then down to 0.5 V (RHE) (figures 2B and 3B). A positive band indicates less absorption in the sample than in the reference potential value, i.e. the species is consumed at the sample potential. According to this a negative band describes the inverse situation, i.e. the species is

formed at the sample potential. The frequency range covered in this investigation extends from 1000 to 3000 cm^{-1}, though no information can be extracted in the region of the bending mode of water at ca. 1640 cm^{-1} [47].

The series of p-polarized spectra plotted in figure 2 exhibit a bipolar wave in the region 2079-2049 cm^{-1} for the potential range 0.2-1.1 V. This feature is apparent only in p-polarization and not in s-polarization (cf. figure 3) and, thus, has to be attributed to surface species. Reference frequency values published in the literature [40,45,46] lead to the assignment of this band to several forms of adsorbed cyanide CN_{ads}. The bipolar character of the band indicates that cyanide is present at both the reference and the sample potentials. The potential dependent frequency shift of the signal then gives rise to an apparent negative and positive absorbance at the frequency corresponding to the reference and the sample potentials, respectively. Absolute cyanide bands can be obtained recalculating the spectra by taking the spectrum recorded at 1.20 V (RHE) as reference, since at that potential value practically all adsorbed cyanide has been removed from the platinum surface. In this way, a negative-going band in the 2060-2100 cm^{-1} range is observed. The potential dependence of the integrated band intensity density for this species is given in figure 4A. During the potential step scan in the positive direction, CN_{ads} is already present on the surface in the range 0.0 – 0.8 V, and the amount of this adsorbate drastically diminishes at more positive potentials becoming zero at 1.5 V. During the potential steps in the negative direction, readsorption occurs for E < 1.0 V describing a maximum at 0.3 V. On the other hand, the small contribution at 2363 cm^{-1} is attributed to CO_2 from the gas phase present in the cabin of the FTIR spectrometer.

Major changes in the spectra are observed when the applied potential becomes more positive than 1.20 V (RHE). Three negative-going bands are observed at 2169, 1607 and 1396 cm^{-1}, which are observable from the spectra recorded with both p-polarized and s-polarized radiation. These bands are also found during the subsequent reversal of the potential at all potential values. From the inspection of the CV in figure 1B, it is observed that the formation of these new features occurs at $E \geq 1.2$ V (RHE) coinciding with the onset of oxygen evolution. The signal at 2169 cm^{-1} appears as a sharp asymmetric peak, the intensity of which grows abruptly up to the most positive potential value considered in this work, and decreases quite slowly as the potential is made more negative during the reverse scan due to the slow diffusion out of the thin layer (cf. figure 4B). The intensities recorded from the integration of this band at each potential value are almost the same for the p-polarized and the s-polarized spectra within the experimental error. The presence of this signal in both series of spectra is an indication that the oxidation product

responsible for this feature remains in the solution phase. This band is attributed to the formation of soluble cyanate [34,40,45,48-50], which is the main electrooxidation product of cyanide in the copper-free alkaline solution. The formation of a surface oxide layer prior to the oxidation of the cyanide ion appears to be a necessary step in the process.

The smaller negative bands observed at 1607 and 1396 cm^{-1}, also appear as result of the major oxidation process occurring for $E \geq 1.2$ V (RHE), though they seem to take place at the expense of the sharp peak recorded at 2078 cm^{-1}. That is, they may be regarded as the result of the partial oxidation of cyanate species. Accordingly, the bands at 1607 and 1396 cm^{-1} could be attributed to the formation of other minor oxidation products such as HCOOH [51] and NO [41], respectively. However, the first feature is rather difficult to assign because this region is greatly affected by the bending vibration of water. The potential dependence of the integrated intensity for the band at 1396 cm^{-1} is given in figure 4C. The shape of the curve is very similar to that obtained for the 2169 cm^{-1} band (cf. figure 4B).

On the other hand, the small band clearly detected at 1.3 V in both p- and s-polarized spectra (see figure 3C for details), can be related to platinum-cyanide complexes, $[Pt(CN)_2]^{2-}$, formed in the oxidation reactions [38]. Finally, the formation of cyanogens species, $(CN)_2$, can be discarded from the inspection of the spectra depicted in figures 2 and 3, since no features are found at its characteristic IR frequency (around 2157 cm^{-1} [52]).

3.3. FTIR spectra in an alkaline solution containing both cyanide and copper ions. Comparison of the FTIR data determined from copper-free and copper-containing cyanide solutions

The corresponding spectra obtained in the alkaline solution containing 23 mM KCN + 8 mM CuCN are shown in figures 5 and 6. Two different potential regions can be defined and compared with the spectra obtained in the absence of copper: the region at $E < 1.1$ V (RHE) and that at $E >$ 1.1 V (RHE). In figure 5, depicting the spectra acquired with p-polarized light, a bipolar band is observed within the former potential range. This band has the positive peak centred at 2074 cm^{-1} and the negative part centred at 2092 cm^{-1}, the latter being a different position compared with that previously shown in figure 3 for the copper-free case. Surprisingly, the same features are depicted in the spectra acquired with s-polarized light given in figure 6, indicating that the nature of the species responsible for these bands is different with respect to those involved in the spectra of figures 3 and 4.That is, a species in the solution has to be involved in this case. The assignment of these bands will be considered later.

For $E > 1.1$ V (RHE), a sharp negative band at 2169 cm^{-1}, associated with the formation of

cyanate, is developed during the positive-going potential excursion as shown in figures 5 and 6. Though this band was also present in figures 3 and 4, the intensity of the band is significantly bigger in the spectra measured in the presence of copper. On the other hand, the negative features observed at 1396 and 1607 cm^{-1} in figures 3 and 4 are not present in these spectra (only a very small contribution is detectable for the contribution at 1396 cm^{-1}). This is an evidence that the reaction path involved in the formation of NO and HCOOH is impeded when copper is present in the electrolyte. Also the band at 2130 cm^{-1} is not observed now.

Additionally, two positive contributions are observed at 2092 and 2074 cm^{-1} with both p-polarized (figure 5) and s-polarized (figure 6) light in this potential range, instead of one single peak at 2078 cm^{-1} detectable with only p-polarized light in the copper-free solution (cf. figures 3 and 4). These features are located at the same positions described for E < 1.1 V (RHE). According to data from the literature [53,54], these bands at 2092 and 2074 cm^{-1} can be attributed to two copper(I)-cyanide complexes, namely $Cu(CN)_3^{2-}$, and $Cu(CN)_4^{3-}$, respectively, which indicates that cyanide ions are participating preferentially in the complexation of the metal ions in the solution phase. For E < 1.1 V (RHE), an equilibrium potential dependence can be established: $Cu(CN)_4^{3-}$ is converted (a positive band of consumption is observed) into $Cu(CN)_3^{2-}$ (a negative band develops). The quantitative formation of cyanate occurs above the onset of oxygen evolution, for E > 1.1 V (RHE), thus requiring oxygen atoms to be available for their oxidation, and leads to the consumption of all copper(I)-cyanide complexes present in the solution at the reference potential, i.e $Cu(CN)_3^{2-}$, and $Cu(CN)_4^{3-}$. The presence of cooper and the formation of these complexes seem to be responsible for the absence of CN_{ads} on the surface. Then, although the onset for cyanide oxidation is maintained, Pt surface places are not blocked and higher currents (correspondingly higher cyanate productions) are detected. In the presence of copper, the formation of $[Pt(CN)_2]^{2-}$ is also impeded.

Another two small bands at 1309 and at 1218 cm^{-1} are observed in the spectra for E > 1.1 V. They have not been referenced in the literature before, and at this stage we tentatively attribute them to the formation of copper(II) species. Furthermore, the band at 1650 cm^{-1} appears in the region of the water bending, and therefore, the assignment to other species is always questionable.

The same bands are observed during the subsequent negative-going potential excursion. The integration of the band for the cyanate feature at 2169 cm^{-1}, and the contributions of the copper-cyanide complexes in the 2092-2074 cm^{-1} range, are plotted as a function of applied potential in

figure 7. These plots show the same trend plots when the sign of the band s is not considered. That is, they exhibit a fast increase of the signal as the potential is set more positive, and they decay very slowly when the potential is made more negative during the reverse potential scan. This behaviour confirms that cyanate formation occurs at the expense of copper-cyanide complexes consumption.

4. Conclusions

Cyanide oxidation at Pt has been studied in alkaline solutions both in the presence of copper and in copper-free solutions. In the absence of copper, two pathways for cyanide oxidation are established. At E < 1.1 V (RHE) (i.e., before the onset of oxygen evolution reaction), cyanide adsorbs on the electrode surface. CN_{ads} is subsequently oxidized when the oxygen reaction commences, with the formation of HCOOH and NO as end products. Once the surface becomes free from the adsorbate, the second reaction occurs: cyanide from the solution becomes oxidized to cyanate by oxygen at the electrode surface. This process takes place at E > 1.1 V (RHE) coinciding with the sharp increase in the current found in the cyclic voltammogram.

The addition of copper ions to the solution results in their complexation with cyanide ions hindering the adsorption of cyanide on the Pt surface. Accordingly, the electrode surface is not poisoned. As the oxidation of cyanide requires oxygen, the onset for this process is not shifted to more negative potentials due to the absence of adspecies, and it is maintained at the onset potential of platinum oxide formation. However, the absence of adsorbates and parallel reactions favours the oxidation of cyanide with the result of a faster current increase in the cyclic voltammograms, and the measurement of higher amounts of cyanate.

Acknowledgements:

The authors are grateful for financial support by the Ministerio de Ciencia e Innovación (Madrid, Spain) in the framework of the contracts CTQ2009-12459, MAT2008-06631-C03-02, and by the Gobierno de Canarias (Consejería de Educación y Deportes, Canary Islands, Spain) under project PI2003/179. This work was initiated within the framework of the Collaborative Research Programme No. HI2004-0297 between Spain and Italy funded by the Ministerio de Educación y Ciencia (Madrid, Spain).

References

(1) Palmer, S. A. K.; Breton, M. A.; Nunno, T. J.; Sullivan, D. M.; Surprenant, N. F. *Metal/cyanide containing wastes*; Noyes Data: New Jersey, 1988.

(2) Monteagudo, J. M.; Rodríguez, I.; Villaseñor, J. ***"Advanced oxidation processes for destruction of cyanide from thermoelectric power station waste waters".*** *J. Chem. Technol. Biotechnol.* **2004**, *79*, 117-125.

(3) Sax, N. I., Ed. *Dangerous Properties of Industrial Materials*, 5th edn.; Van Nostrand-Reinhold: New York, 1979, p. 526.

(4) Ramaldo, R. S. *Introduction to Wastewater Treatment Processes*, 2nd edn.; Academic Press: New York, 1983, p. 533.

(5) Eckenfelder, W. W. *Industrial Water Pollution Control*, 2nd edn.; McGraw-Hill: New York, 1989, p. 303.

(6) Szpyrkowicz, L.; Ricci, F.; Daniele, S. *Proceedings of Indo-Italian Workshop on Emerging Technologies for Industrial Wastewater and Environment* **2002**, 58-65.

(7) Lu, J., Dreisinger, D. B.; Cooper, W. C. *Hydrometallurgy* **2002**, *66*, 23-36.

(8) Tamura, T.; Arikado, T.; Yoneyama, H.; Matsuda, Y. *Electrochim. Acta* **1974**, *19*, 273-277.

(9) Arikado, T.; Iwakura, C.; Yoneyama, H.; Tamura, H. *Electrochim. Acta* **1976**, *21*, 1021-1027.

(10) Tan, T. C.; Teo, W. K.; Chin, D. T. *Chem. Eng. Commun.* **1985**, *38*, 125-133.

(11) Hine, F.; Yasuda, M.; Iida, T.; Ogata, Y. *Electrochim. Acta* **1986**, *31*, 1389-1395.

(12) Kelsall, G. H.; Savage, S.; Brandt, D. *J. Electrochem. Soc.* **1991**, *138*, 117-124.

(13) Bergmann, H.; Hertwig, H.; Nieber, F. *Chem. Eng. Processes* **1992**, *31*, 195-203.

(14) Tissot, P.; Fragniére, M. *J. Appl. Electrochem.* **1994**, *24*, 509-512.

(15) Buso, A.; Giomo, M.; Boaretto, L.; Sandoná, G.; Paratella, A. *Chem. Eng. Processes* **1997**, *36*, 255-260.

(16) Bakir Ögütveren, Ü.; Törü, E.; Koparal, S. *Water Res.* **1999**, *33*, 1851-1856.

(17) Cañizares, P.; Díaz, M.; Domínguez, J. A.; Lobato, J.; Rodrigo, M. A. *J.Chem.*

Technol. Biotechnol. **2005**, *80*, 565-573.

(18) Szpyrkowicz, L.; Kelsall, G. H.; Souto, R. M.; Ricci, F.; Kaul, S. N. *Chem. Eng. Sci.* **2005**, *60*, 523-533.

(19) El-Ghaoui, E. A.; Jansson, R. E. *J. Appl. Electrochem.* **1982**, *12*, 69-73.

(20) Ho, S. P.; Y.Y. Wang and C.C. Wan, *Water Res.* **1990**, *24*, 1317-1321.

(21) Wels, B.; Johnson, D. C. *J. Electrochem. Soc.* **1990**, *137*, 2785-2791.

(22) Hofseth, C. S.; Chapman, T. W. *J. Electrochem. Soc.* **1999**, *146*, 199-207.

(23) Hofseth, C. S.; Chapman, T. W. *J. Electrochem. Soc.* **1991**, *138*, 2321-2327.

(24) Lin, M. L.; Wang, Y. Y.; Wan, C. C. *J. Appl. Electrochem.* **1992**, *22*, 1197-1200.

(25) Szpyrkowicz, L.; Zilio-Grandi, F.; Kaul, S. N.; Rigoni-Stern, S. *Water Sci. Technol.* **1998**, *38*, 261-268.

(26) Szpyrkowicz, L.; Kaul, S. N.; Molga, E.; DeFaveri, M. *Electrochim. Acta* **2000**, *46*, 381-387.

(27) Szpyrkowicz, L.; Kelsall, G. H.; Souto, R. M.; Ricci, F.; Kaul, S. N. *Chem. Eng. Sci.* **2005**, *60***,** 535-543.

(28) Hwang, J.- Y.; Hwang, Y.- Y.; Wan, C. C. *J. Appl. Electrochem.* **1987**, *17*, 684-694.

(29) Casella, I. G.; Gatta, M. *J. Electroanal. Chem.* **2000**, *494*, 12-20.

(30) Cheng, S.C.; Gatrell, M.; Guena, T.; MacDougall, B. *Electrochim. Acta* **2002**, *47*, 3245-3256.

(31) Szpyrkowicz, L.; Ricci, F.; Montemor, M. F.; Souto, R. M. *J. Hazardous Mater. B* **2005**, *119***,** 145-152.

(32) Katagiri, A.; Yoshimura, S.; Yoshizawa, S. *Inorg. Chem.* **1981**, *20*, 4143-4147.

(33) Reyes-Cruz, V.; González, I.; Oropeza, M. T. *J. Solid State Electrochem.* **2005**, *9*, 566-573.

(34) Kitamura, F.; Takahashi, M.; Ito, M. *Chem. Phys. Letters* **1986**, *130*, 181-184.

(35) Kitamura, F.; Takahashi, M.; Ito, M. *Chem. Phys. Letters* **1987**, *136*, 62-66.

(36) Ashley, K.; Weinert, F.; Feldheim, D. L. *Electrochim. Acta* **1991**, *36*, 1863-1868.

(37) Ashley, K.; Weinert, F.; Samant, M. G.; Seki, H.; Philpott, M. R. *J. Phys. Chem.* **1991**, *95*, 7409-7414.

(38) Kim, C. S.; Korzeniewski, C. *J. Phys. Chem.* **1993,** *97*, 9784-9787.

(39) Stuhlmann, C.; Villegas, I.; Weaver, M. J. *Chem. Phys. Letters* **1994**, *219*, 319-324.

(40) Ashley, K.; Feldheim, D. L.; Barry, D. B.; Samant, M. G.; Philpott, M. R. *J. Electroanal. Chem.* **1994**, *373*, 201-209.

(41) Huerta, F. J.; Morallón, E.; Vázquez, J. L.; Aldaz, A. *Surf. Sci.* **1998**, *396*, 400-410.

(42) Iwasita, T.; Nart, F. C. in: *Advances in Electrochemical Science and Engineering*, Vol. 4, Gerischer H., Tobias, C. W. , Eds.; VCH: New York, 1995, p. 123.

(43) Iwasita, T.; Nart, F. C. *Prog. Surf. Sci.* **1997**, *55*, 271-340.

(44) Ashley, K.; Samant, M. G.; Seki, H.; Philpott, M. R. *J. Electroanal. Chem.* **1989**, *270*, 349-364.

(45) Paulissen V. B.; Korzeniewski, C. *J. Phys. Chem.* **1992**, *96*, 4563-4567.

(46) Tadjeddine A.; Guyot-Sionnest, P. *Electrochim. Acta* **1991**, *36*, 1839-1847.

(47) Nakamoto, K. *Infrared and Raman Spectra of Inorganic and Coordination Compounds*; Wiley: New York, 1997.

(48) Yépez, O.; Scharifker, B. R. *Electrochim. Acta* **2005**, *50*, 1423-1429.

(49) Hinman, A. S.; Kydd, R. A.; Cooney, R. P. *J. Chem. Soc. Faraday Trans.I* **1986**, *82*, 3525-3534.

(50) Roth, J. D.; Weaver, M. J. *Anal. Chem.* **1991**, *63*, 1603-1606.

(51) Li, H.- Q.; Chen, A.; Roscoe, S. G.; Lipkowski, J. *J. Electroanal. Chem.* **2001**, *500*, 299-310.

(52) Craine, G. D.; Thomsen, H. W. *Trans. Faraday Soc.* **1953**, *49*, 1273-1280.

(53) Lee, K. A. B.; Kunimatsu, K.; Gordon, J. G.; Golden, W. G.; Seki, H. *J. Electrochem. Soc.* **1987**, *134*, 1676-1678.

(54) Johnson, P. J.; Harach, D. J. *Hydrometallurgy* **2004**, *74*, 67-75.

Figure captions:

Figure 1 - Voltammetric profiles of a platinum electrode in alkaline aqueous solution (pH 13). (A) base electrolyte, (B) base electrolyte + 31 mM KCN; (C) base electrolyte + 23 mM KCN + 8 mM CuCN. v = 0.1 V s^{-1}.

Figure 2 - In situ FTIR spectra of Pt in the alkaline solution containing 31 mM KCN (p-polarized radiation) as a function of electrode potential. E_0 = 0.05 V (RHE). Potential steps first in the positive-going direction (A) and then in the negative-going direction (B). The potential values indicated in the figure are referred to the RHE.

Figure 3 - In situ FTIR spectra of Pt in the alkaline solution containing 31 mM KCN (s-polarized radiation) as a function of electrode potential. E_0 = 0.05 V (RHE). Potential steps first in the positive-going direction (A) and then in the negative-going direction (B). (C) Detail of the spectrum for E = 1.3 V (RHE). The potential values indicated in the figure are referred to the RHE.

Figure 4 - Potential dependence of the integrated band intensities for the different chemical processes observed in Figure 3. Features observed (A) in the 2060-2100 cm^{-1} range, (B) at 2169 cm^{-1}, and (C) at 1396 cm^{-1}.

Figure 5 - *In situ* FTIR spectra of Pt in the alkaline solution containing 23 mM KCN + 8 mM CuCN (p-polarized radiation) as a function of electrode potential. Potential steps first in the positive-going direction (A) and then in the negative-going direction (B). E_0 = 0.05 V (RHE). The potential values indicated in the figure are referred to the RHE.

Figure 6 - *In situ* FTIR spectra of Pt in the alkaline solution containing 23 mM KCN + 8 mM CuCN (s-polarized radiation) as a function of electrode potential. Potential steps first in the positive-going direction (A) and then in the negative-going direction (B). E_0 = 0.05 V (RHE). The potential values indicated in the figure are referred to the RHE.

Figure 7 - Potential dependence of the integrated band intensities for the different chemical processes observed in figure 6. Feature s observed (A) at 2169 cm^{-1}, and (B) in the 2092-2074 cm^{-1} range.

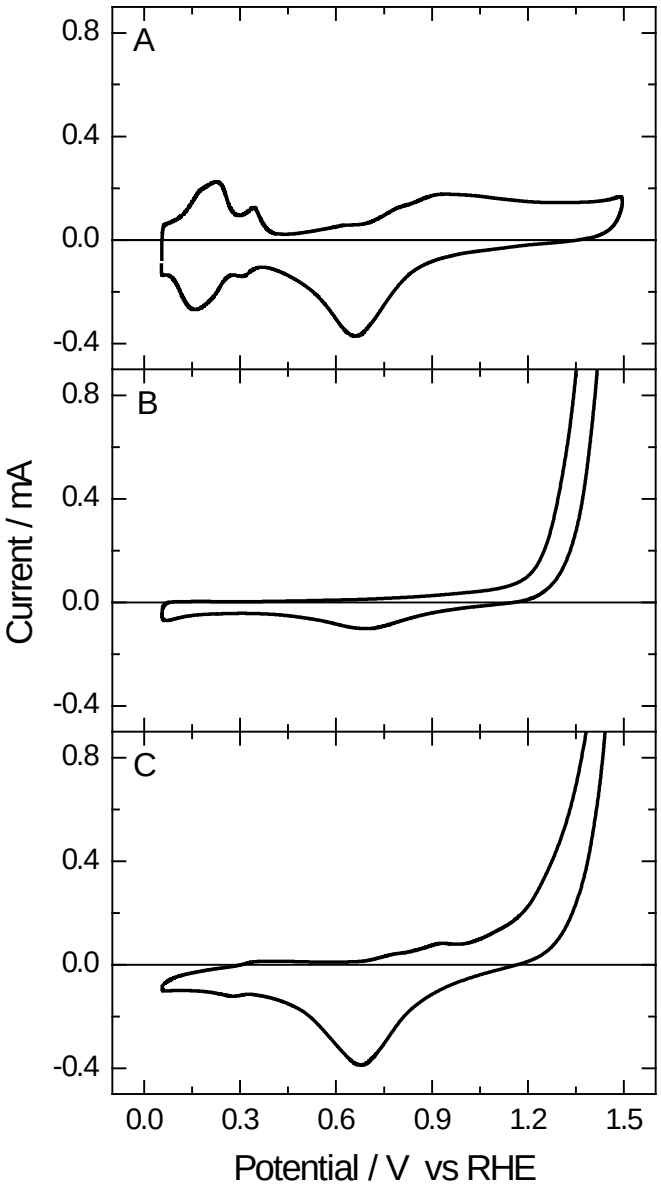

Souto et al.

Figure 1

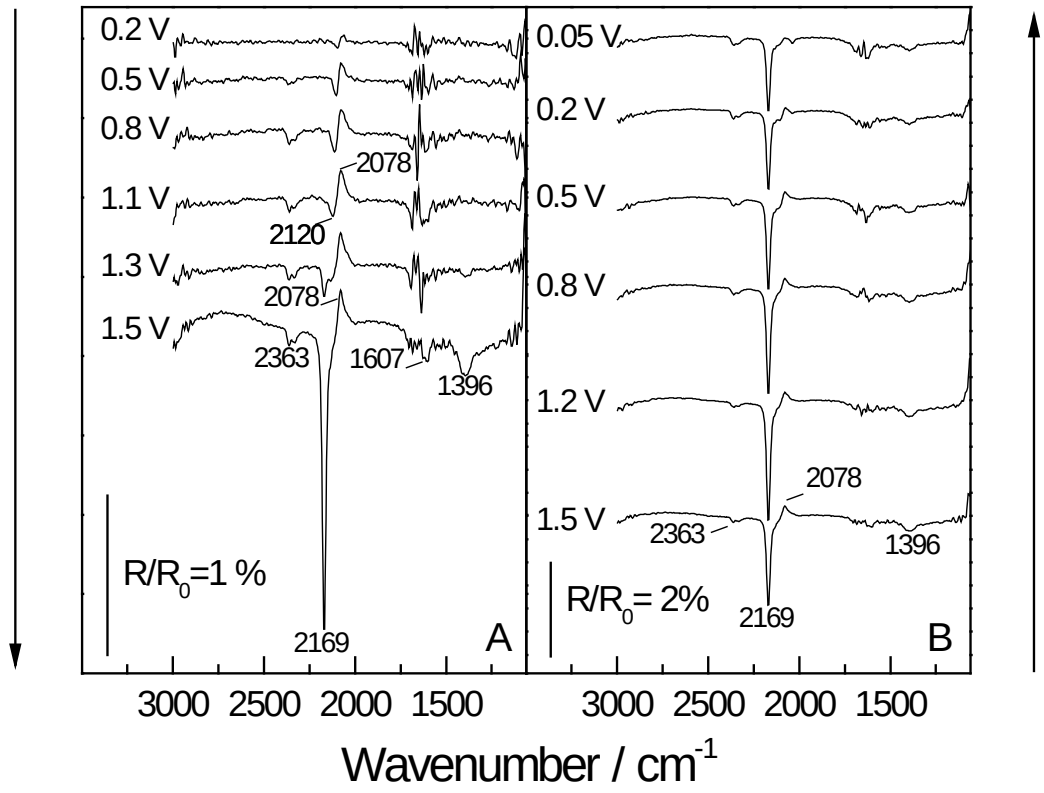

Souto et al.

Figure 2

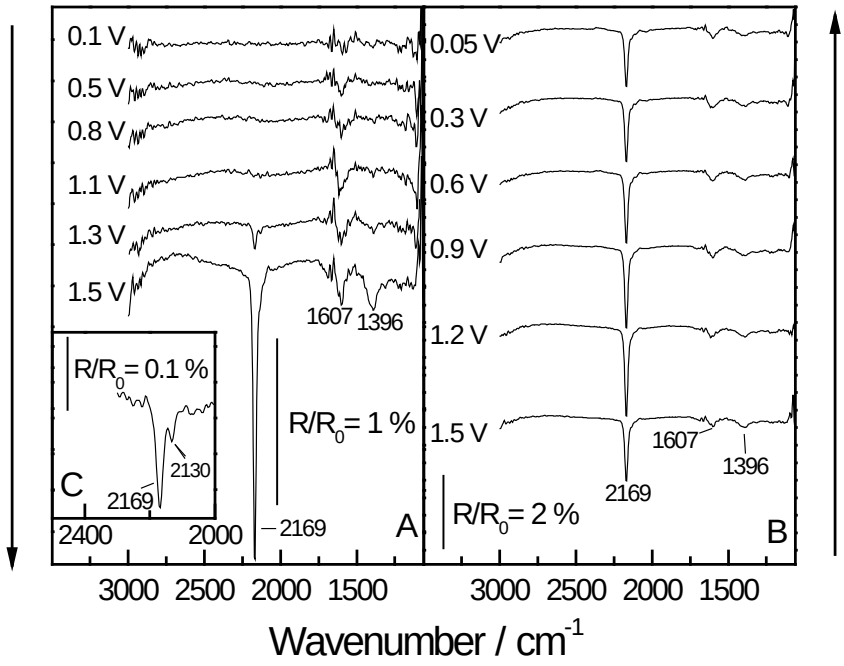

Souto et al.

Figure 3

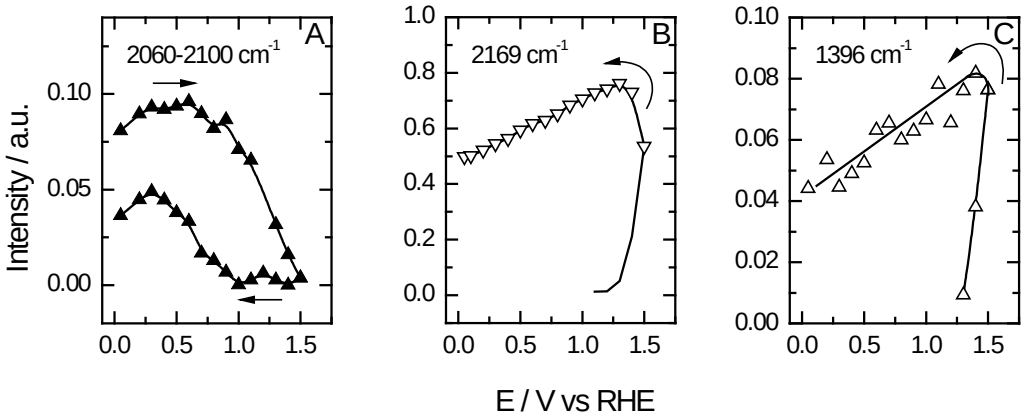

Souto et al.

Figure 4

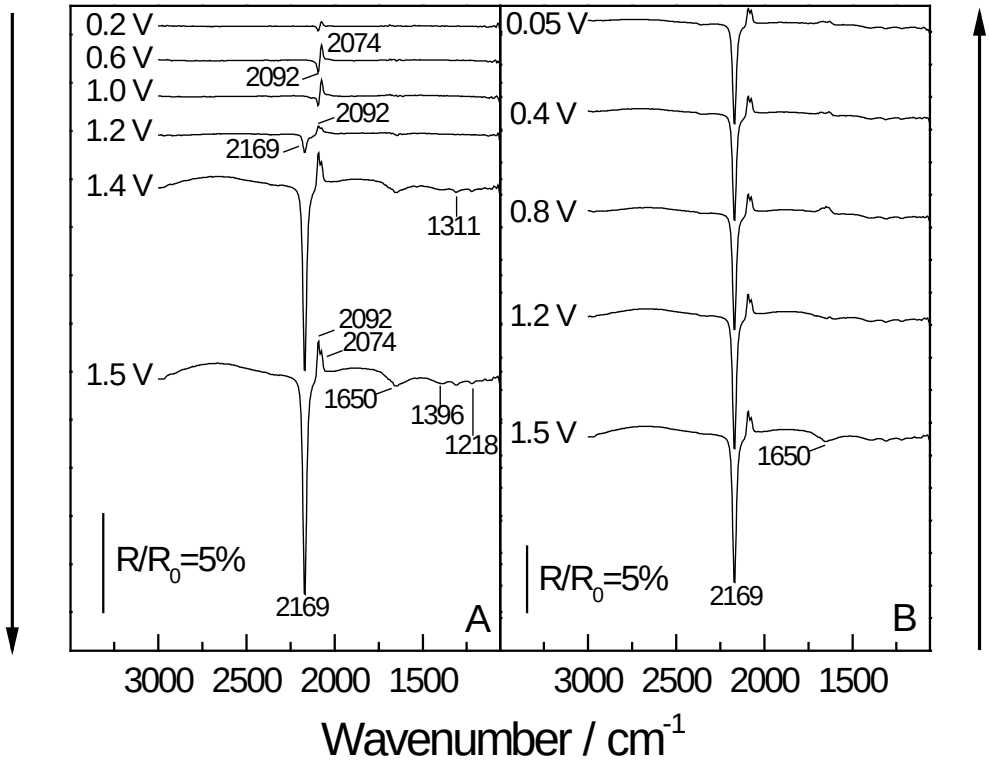

Souto et al.

Figure 5

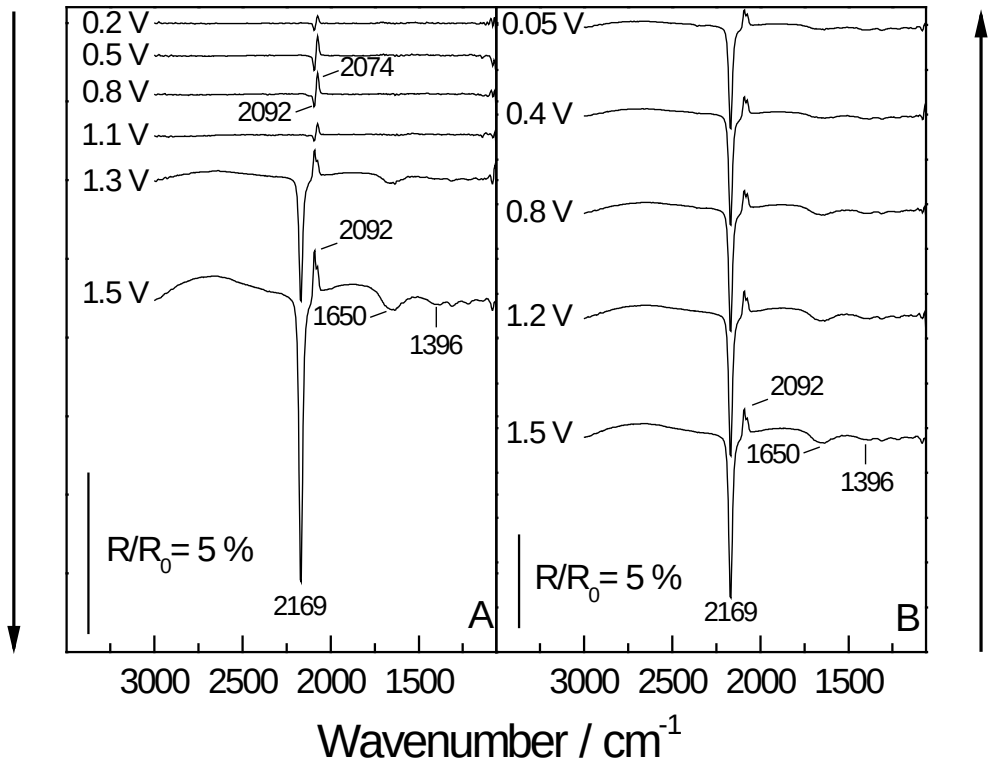

Souto et al.

Figure 6

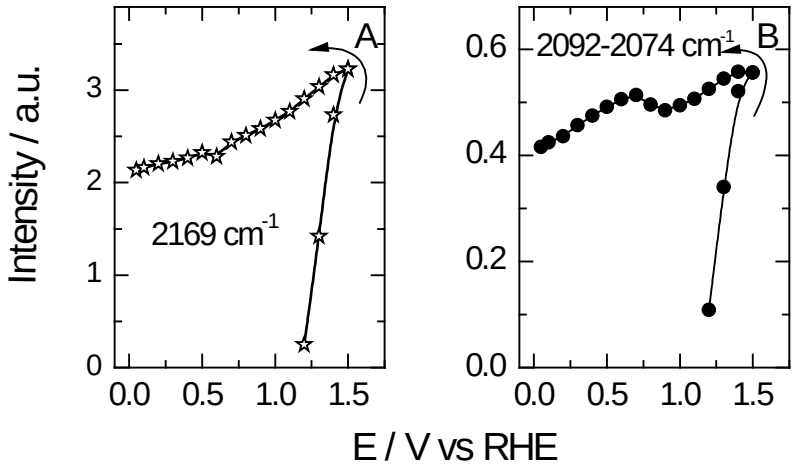

Souto et al.

Figure 7